arXiv:cond-mat/0110197v1 [cond-mat.str-el] 10 Oct 2001

Charge and Orbital Ordering in the Triangular-Lattice t_{2g}-Orbital System in One Dimension: A Possible Ground State of $\mathrm{Bi}_x\mathrm{V}_8\mathrm{O}_{16}$

Yoshinori Shibata[1] * and Yukinori Ohta[1,2] **

[1] *Graduate School of Science and Technology, Chiba University, Chiba 263-8522*
[2] *Department of Physics, Chiba University, Chiba 263-8522*

(Received September 25, 2001)

We consider the possible charge and orbital ordering in a Hollandite compound $\mathrm{Bi}_x\mathrm{V}_8\mathrm{O}_{16}$, which is a new one-dimensional triangular-lattice t_{2g}-orbital system. Using the strong-coupling perturbation theory, we derive the effective spin-orbit Hamiltonian in the approximation neglecting the small off-diagonal hopping parameters or orbital fluctuation, whereby we obtain the spin Hamiltonians in the partial space of each orbital-ordering pattern. We then apply an exact-diagonalization technique on small clusters to these spin Hamiltonians and calculate the ground-state phase diagram. We find that a variety of orbital-ordering patterns appear in the parameter space, which include the state characterized by the partial singlet formation consistent with recent NMR experiment.

KEYWORDS: charge ordering, orbital ordering, vanadate, Hollandite, $\mathrm{Bi}_x\mathrm{V}_8\mathrm{O}_{16}$, perturbation theory

§1. Introduction

Orbital physics in transition-metal oxides, such as the orbital ordering (OO) of the e_g-spins of Mn-oxides, has attracted much attention in the research field of strongly correlated electron systems.[1)] Recently, Kato *et al.*[2)] measured the magnetic susceptibility and resistivity of $\mathrm{Bi}_x\mathrm{V}_8\mathrm{O}_{16}$ with $1.72 < x < 1.8$ and found a metal-insulator transition (MIT) at $T < 80$ K. The crystal structure of this compound belongs to a group of Hollandite-type phases and has a $\mathrm{V}_8\mathrm{O}_{16}$ framework composed of double strings of edge-shared VO_6 octahedra as shown in Fig. 1. Kato *et al.*[2)] suggested a mechanism of the transition that the charge ordering (CO) between V^{3+} and V^{4+} accompanied by an OO occurs with MIT.

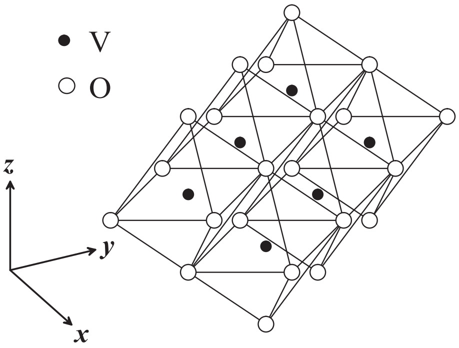

Fig. 1. Schematic representation of the double string of edge-shared VO_6 octahedra in $\mathrm{Bi}_x\mathrm{V}_8\mathrm{O}_{16}$.

In the viewpoint of orbital physics, this system may be regarded as a one-dimensional (1D) version of LiVO_2 known as a possible OO system of t_{2g}-orbitals on the 2D triangular lattice of $S = 1$ spins,[3,4)] although our system $\mathrm{Bi}_x\mathrm{V}_8\mathrm{O}_{16}$ has the average valence of $\mathrm{V}^{(3+1/3)+}$ at $x = 16/9$ and thus is in the mixed valent state of $\mathrm{V}^{3+} : \mathrm{V}^{4+} = 3d^2 : 3d^1 = 2 : 1$.[2)] The central issue in the present system is therefore the mechanism of the MIT concerning how the highly frustrated spin, charge, and orbital degrees of freedom at high temperatures are relaxed by lowering temperatures and what type of the ground state is realized at zero temperature.

To consider this issue, we study in this paper the possible ground state of this system. We thereby assume that the V-ions, which have the triply degenerate t_{2g}-orbitals with intra- and inter-orbital Coulomb interactions as well as Hund's rule coupling, form the 1D triangular lattice and that the intersite Coulomb repulsions are strong enough for the electrons to be localized to form a spatial CO pattern. We then use the strong-coupling perturbation theory[5)] to derive the effective spin-orbit Hamiltonian, which turns out to be block-diagonal with vanishing orbital-off-diagonal elements within the approximation used. We employ a numerical exact-diagonalization technique on small clusters of this Hamiltonian to consider the possible OO spatial patterns in the ground state. We find that a variety of the ground-state phases appear in the parameter space. We also discuss the spin degrees of freedom of the obtained OO patterns. We argue that the state characterized by the singlet formation of two $S = 1$ spins on the neighboring V^{3+}-ions with remaining nearly-free $S = 1/2$ spins on the V^{4+}-ions might be relevant in the present material.

Although the experimental data on this new system $\mathrm{Bi}_x\mathrm{V}_8\mathrm{O}_{16}$ are quite limited at present, we hope that our

---

* E-mail: shibata@physics.s.chiba-u.ac.jp

** E-mail: ohta@science.s.chiba-u.ac.jp

first theoretical study on its charge, orbital, and spin degrees of freedom would stimulate further experimental studies of this intriguing material.

§2. Model

Our starting high-energy Hamiltonian is of the following form:

$$\begin{aligned} H &= H_0 + H_t \\ H_0 &= V \sum_{\langle ij \rangle} n_i n_j - J_H \sum_{i\sigma\sigma',\alpha\neq\beta} c^{\dagger}_{i\alpha\sigma} c^{\dagger}_{i\beta\sigma'} c_{i\beta\sigma} c_{i\alpha\sigma'} \\ &\quad + U' \sum_{i,\alpha\neq\beta} n_{i\alpha} n_{i\beta} + U \sum_{i\alpha} n_{i\alpha\uparrow} n_{i\alpha\downarrow} \\ H_t &= - \sum_{\langle i\alpha, j\beta \rangle,\sigma} t_{i\alpha,j\beta} (c^{\dagger}_{i\alpha\sigma} c_{j\beta\sigma} + \mathrm{H.c.}) \end{aligned}$$

where V is the intersite Coulomb repulsion, J_H is the Hund's rule coupling, and U and U' are the intra- and inter-orbital Coulomb repulsions, respectively. $\langle \cdots \rangle$ stands for the nearest-neighbor pair of sites. We neglect the crystal-field splittings among the t_{2g}-orbitals for simplicity because the gain in kinetic energy may be much larger than the splittings as has been assumed in ref.[3] We also assume the relation $U' = U - 2J_H$, which is valid in the atomic limit.[6] $t_{i\alpha,j\beta}$ is the hopping parameter between the orbital α on site i and orbital β on site j where $\alpha, \beta \in \{d_{xy}, d_{yz}, d_{zx}\}$ in the coordinate system shown in Fig. 1. We retain the direct hoppings between the t_{2g}-orbitals on the V-ions because the indirect hoppings via the O-ions are rather small.[3] Independent nearest-neighbor $t_{i\alpha,j\beta}$ parameters are t_a, t_b, and t_c as shown in Fig. 2. $c^{\dagger}_{i\alpha\sigma}$ $(c_{i\alpha\sigma})$ is the electron creation (annihilation) operator at site i, orbital α, and spin σ, and $n_{i\alpha\sigma} = c^{\dagger}_{i\alpha\sigma} c_{i\alpha\sigma}$ is the number operator. We also define $n_{i\alpha} = n_{i\alpha\uparrow} + n_{i\alpha\downarrow}$ with $\sigma = \uparrow, \downarrow$ and $n_i = \sum_\alpha n_{i\alpha}$.

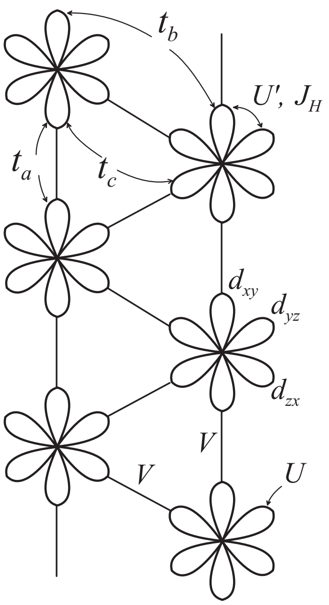

Fig. 2. Schematic representation of the t_{2g}-orbitals on the 1D triangular lattice. Two of the four lobes for each of the three t_{2g}-orbitals are drawn.

§3. Charge ordering

First, we consider the CO in the ground state. We assume the limit of no doubly occupied orbitals. Then, if we assume that the inter-site Coulomb repulsions V (as well as the inter-orbital Coulomb repulsion U') is much larger than the hopping parameters, we find the ground state of the system to be charge ordered. It is readily noticed that the lowest-energy CO state has the ordered pattern like $\cdots V^{3+}V^{3+}V^{4+} \cdots$ as shown in Fig. 3. At $H_t = 0$, this state has the ground-state energy

$$E_0 = \frac{N}{6}(4U' - 4J_H + 32V)$$

when there are no doubly occupied orbitals, whereas the states containing V^{2+} or V^{5+} have the ground-state energy

$$E_0 = \frac{N}{6}(6U' - 6J_H + 28V)$$

for $\cdots \mathrm{V}^{2+}\mathrm{V}^{4+}\mathrm{V}^{4+} \cdots$, and

$$E_0 = \frac{N}{6}(8U' - 8J_H + 24V)$$

for $\cdots \mathrm{V}^{2+}\mathrm{V}^{3+}\mathrm{V}^{5+} \cdots$. Since the states containing V^{2+} or V^{5+} are highly unrealistic, we should have the condition

$$U' - 2V - J_H > 0$$

for the presence of CO of only V^{3+} and V^{4+} ions.

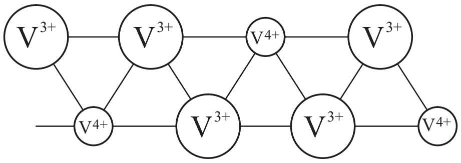

Fig. 3. Schematic representation of the CO pattern in the 1D triangular lattice.

The ground state of the unperturbed ($H_t = 0$) Hamiltonian is then of the degeneracy

$$M = 3^N \cdot 3^{2N/3} \cdot 2^{N/3}$$

because there are 3^N choices of orbitals, $3^{2N/3}$ choices of $S = 1$ spins, and $2^{N/3}$ choices of $S = 1/2$ spins, where N is the number of sites in the system. The degeneracy is lifted by the perturbation of small hopping parameters $t_{i\alpha,j\beta}$ as shown in the next section.

§4. Effective Hamiltonian

We carry out the second-order perturbation calculation with respect to $t_{i\alpha,j\beta}$ assuming that $t_{i\alpha,j\beta}$ is much smaller than U, U', and V. The degeneracy is lifted by the perturbation and the effective spin-orbit Hamiltonian is obtained as follows:

$$H_{\mathrm{eff}} = H_0 - \sum_{\mu\mu'} |\mu\rangle \sum_n \frac{\langle\mu|H_t|n\rangle\langle n|H_t|\mu'\rangle}{E_n - E_0} \langle\mu'|$$

where $|\mu\rangle$ and $|\mu\rangle'$ ($\mu, \mu' = 1, \cdots, M$) are the M independent eigenvectors of the ground state of H_0 and $|n\rangle$ are the n-th excited states of H_0. E_0 and E_n are the corresponding eigenenegies of H_0.

To find the expressions for the effective Hamiltonian, let us first prepare the degenerate eigenstates of H_0:

$$|\psi_0\rangle = \sum_{\{q\}} C(\{q\}) \prod_i |s_i, s_i^z, n_i, n_i^d\rangle_{\{\alpha_i\}}$$

where s_i and s_i^z are the spin quantum numbers at site-i, n_i is the number of electrons at site-i, n_i^d is the number of doubly occupied orbitals at site-i, and $\{\alpha_i\}$ is the set of occupied orbitals. $\{q\}$ represents a set of all these qantum numbers. The basis states $|s_i, s_i^z, n_i, n_i^d\rangle_{\{\alpha_i\}}$ may be of the following form:

(i) For the d^1-site, we have

$$|1/2, 1/2, 1, 0\rangle_\alpha = |\uparrow\rangle_\alpha$$
$$|1/2, -1/2, 1, 0\rangle_\alpha = |\downarrow\rangle_\alpha$$

with $S = 1/2$ and $\alpha = xy$, yz, zx.

(ii) For the d^2-site, we have

$$|1, 1, 2, 0\rangle_{\alpha\beta} = |\uparrow\rangle_\alpha |\uparrow\rangle_\beta$$
$$|1, 0, 2, 0\rangle_{\alpha\beta} = \frac{1}{\sqrt{2}}(|\uparrow\rangle_\alpha |\downarrow\rangle_\beta + |\downarrow\rangle_\alpha |\uparrow\rangle_\beta)$$
$$|1, -1, 2, 0\rangle_{\alpha\beta} = |\downarrow\rangle_\alpha |\downarrow\rangle_\beta$$

for $S = 1$, and

$$|0, 0, 2, 0\rangle_{\alpha\beta} = \frac{1}{\sqrt{2}}(|\uparrow\rangle_\alpha |\downarrow\rangle_\beta - |\downarrow\rangle_\alpha |\uparrow\rangle_\beta)$$
$$|0, 0, 2, 1\rangle_\alpha = |d\rangle_\alpha$$

for $S = 0$, where d means the double occupancy.

(iii) For the d^3-site, we have

$$|3/2, 3/2, 3, 0\rangle_{\alpha\beta\gamma} = |\uparrow\uparrow\uparrow\rangle$$
$$|3/2, 1/2, 3, 0\rangle_{\alpha\beta\gamma} = \frac{1}{\sqrt{3}}(|\uparrow\uparrow\downarrow\rangle + |\uparrow\downarrow\uparrow\rangle + |\downarrow\uparrow\uparrow\rangle)$$
$$|3/2, -1/2, 3, 0\rangle_{\alpha\beta\gamma} = \frac{1}{\sqrt{3}}(|\downarrow\downarrow\uparrow\rangle + |\downarrow\uparrow\downarrow\rangle + |\uparrow\downarrow\downarrow\rangle)$$
$$|3/2, -3/2, 3, 0\rangle_{\alpha\beta\gamma} = |\downarrow\downarrow\downarrow\rangle$$

for $S = 3/2$, and

$$|1/2, 1/2, 3, 0\rangle^{(1)}_{\alpha\beta\gamma} = \frac{1}{\sqrt{2}}(|\uparrow\downarrow\uparrow\rangle - |\downarrow\uparrow\uparrow\rangle)$$
$$|1/2, 1/2, 3, 0\rangle^{(2)}_{\alpha\beta\gamma} = \frac{1}{\sqrt{5}}(|\uparrow\downarrow\uparrow\rangle + |\downarrow\uparrow\uparrow\rangle - 2|\uparrow\uparrow\downarrow\rangle)$$
$$|1/2, 1/2, 3, 1\rangle_{\alpha\beta} = |d\rangle_\alpha |\uparrow\rangle_\beta$$
$$|1/2, -1/2, 3, 0\rangle^{(1)}_{\alpha\beta\gamma} = \frac{1}{\sqrt{2}}(|\uparrow\downarrow\downarrow\rangle - |\downarrow\uparrow\downarrow\rangle)$$
$$|1/2, -1/2, 3, 0\rangle^{(2)}_{\alpha\beta\gamma} = \frac{1}{\sqrt{5}}(|\uparrow\downarrow\downarrow\rangle + |\downarrow\uparrow\downarrow\rangle - 2|\downarrow\downarrow\uparrow\rangle)$$
$$|1/2, -1/2, 3, 1\rangle_{\alpha\beta} = |d\rangle_\alpha |\downarrow\rangle_\beta$$

for $S = 1/2$, where we use the notation $|\sigma_1\sigma_2\sigma_3\rangle = |\sigma_1\rangle_\alpha |\sigma_2\rangle_\beta |\sigma_3\rangle_\gamma$. These states are used in the following as the intermediate states of the second-order perturbation processes.

We here introduce an approximation; because the hopping parameters $t_{i\alpha,j\beta}$ take the values $t_a \gg t_b \simeq t_c$,[3)] we assume $t_b = t_c = 0$ for simplicity as in ref.[3)] This means that the terms like $H_{ij}^{\mathrm{eff}} \propto t_a t_c$ and $H_{ij}^{\mathrm{eff}} \propto t_b t_c$ are all neglected, retaining only the terms like $H_{ij}^{\mathrm{eff}} \propto t_a^2$ in the second-order processes. We note that the orbital fluctuations are completely suppressed in this approximation because only two orbitals connected with the *diagonal* hopping t_a comes out and no *off-diagonal* hopping terms appear in the effectve Hamiltonian. In other words, we obtain the effective spin-orbit Hamiltonian consisting of orbital-diagonal spin-sub-blocks with vanishing orbital off-diagonal blocks.

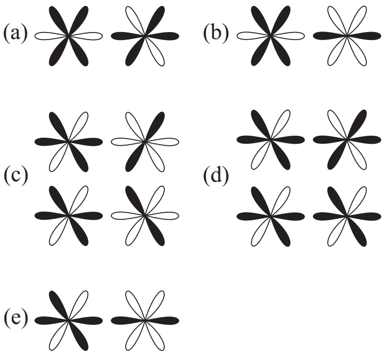

Fig. 4. Schematic representation of five types of the bonds with different exchange interactions. (a) FM-1: the ferromagnetic bond with the process $d_i^2 d_j^2 \to d_i^3 d_j^1 \to d_i^2 d_j^2$, (b) FM-2: the ferromagnetic bond with the process $d_i^2 d_j^1 \to d_i^3 d_j^0 \to d_i^2 d_j^1$, (c) FM-3: the ferromagnetic bond with the process $d_i^2 d_j^1 \to d_i^1 d_j^2 \to d_i^2 d_j^1$, (d) AF-1: the antiferromagnetic bond with the process $d_i^2 d_j^2 \to d_i^3 d_j^1$ or $d_i^1 d_j^3 \to d_i^2 d_j^2$, and (e) AF-2: the antiferromagnetic bond with the process $d_i^2 d_j^1 \to d_i^3 d_j^0$ or $d_i^1 d_j^2 \to d_i^2 d_j^1$.

We then have five types of bonds of spin exchange interactions as shown in Fig. 4; three of them are the bonds with ferromagnetic (FM) exchange interaction due to double-exchange mechanism and two of them are the bonds with antiferromagnetic (AF) exchange interaction due to kinetic-exchange mechanism. Defining the spin-1 operator as $\mathbf{S}_i$ and spin-1/2 operator as $\mathbf{s}_i$, we have the following Hamiltonian for each bond shown in Fig. 4.

(i) The bond FM-1 with the process $d_i^2 d_j^2 \to d_i^3 d_j^1 \to d_i^2 d_j^2$:

$$H_{ij}^{\mathrm{eff}} = -J\mathbf{S}_i \cdot \mathbf{S}_j + c\hat{1}$$
$$J = \frac{t_a^2}{3(U' - V - J_H)} - \frac{2t_a^2}{5(U' - V + 2J_H)}$$

$$c = -\frac{2t_a^2}{3(U' - V - J_H)} - \frac{2t_a^2}{5(U' - V + 2J_H)}$$

where $\hat{1}$ is the unit operator.

(ii) The bond FM-2 with the process $d_i^2 d_j^1 \to d_i^3 d_j^0 \to d_i^2 d_j^1$:

$$H_{ij}^{\mathrm{eff}} = -2J\mathbf{S}_i \cdot \mathbf{s}_j + c\hat{1}$$

$$J = \frac{t_a^2}{3(2U' - 3V - 2J_H)} - \frac{2t_a^2}{5(2U' - 3V + J_H)}$$

$$c = -\frac{2t_a^2}{3(2U' - 3V - 2J_H)} - \frac{2t_a^2}{5(2U' - 3V + J_H)}$$

(iii) The bond FM-3 with the process $d_i^2 d_j^1 \to d_i^1 d_j^2 \to d_i^2 d_j^1$:

$$H_{ij}^{\mathrm{eff}} = -2J\mathbf{S}_i \cdot \mathbf{s}_j + c\hat{1}$$

$$J = \frac{t_a^2}{4V} - \frac{t_a^2}{4(V + 2J_H)}$$

$$c = -\frac{3t_a^2}{4V} - \frac{t_a^2}{4(V + 2J_H)}$$

In the above three, we have the competing exchange couplings with positive and negative sign, but the sum is always positive for realistic values of the parameters J_H, V, and U'.

(iv) The bond AF-1 with the process $d_i^2 d_j^2 \to d_i^3 d_j^1$ or $d_i^1 d_j^3 \to d_i^2 d_j^2$:

$$H_{ij}^{\mathrm{eff}} = J\mathbf{S}_i \cdot \mathbf{S}_j + c\hat{1}$$

$$J = -c = \frac{t_a^2}{U - V + J_H}$$

(v) The bond AF-2 with the process $d_i^2 d_j^1 \to d_i^3 d_j^0$ or $d_i^1 d_j^2 \to d_i^2 d_j^1$:

$$H_{ij}^{\mathrm{eff}} = 2J\mathbf{S}_i \cdot \mathbf{s}_j + c\hat{1}$$

$$J = -c = \frac{t_a^2}{2(U + U' - 3V)} + \frac{t_a^2}{2(U - U' + V + J_H)}$$

These two exchange couplings have the doubly occupied states in their intermediate state and thus they are antiferromagnetic.

Note that the intersite Coulomb repulsion V can be included in the bond Hamiltonian as shown above because, due to the fixed CO pattern of Fig. 3, all the intermediate states have the same intersite Coulomb energy, irrespective of the location of the bond. Also noted is that the so-called three-site terms in the perturbation do not appear for the CO pattern to be fixed.

Thus, we have the effective spin-orbit Hamiltonian

$$H_{\mathrm{eff}} = \sum_{<ij>} H_{ij}^{\mathrm{eff}}$$

where the sum runs over all the nearest-neighbor pairs of sites. Note that this effective spin-orbit Hamiltonian has the form of block-diagonal in the spin$\otimes$orbit space; i.e., orbital off-diagonal blocks are all zero. In other words, we have 3^N OO patterns for the N-site systems, and for each of them, we have the spin Hamiltonian. If we diagonalize all the spin Hamiltonians, we can obtain the eigenstates of our effective spin-orbit Hamiltonian. We use the Lanczos diagonalization technique on small clusters to diagonalize the spin sub-block Hamiltonians and by comparing the lowest enrgies obtained we find the ground-state OO patterns in the parameter space.

Table I. Number of bonds in each OO pattern calculated for the 12-site cluster.

type of bond	phase-I	phase-II	phase-III	phase-IV
FM-1	4	2	0	6
FM-2	4	2	0	4
FM-3	12	12	12	10
AF-1	4	4	4	2
AF-2	0	2	4	2

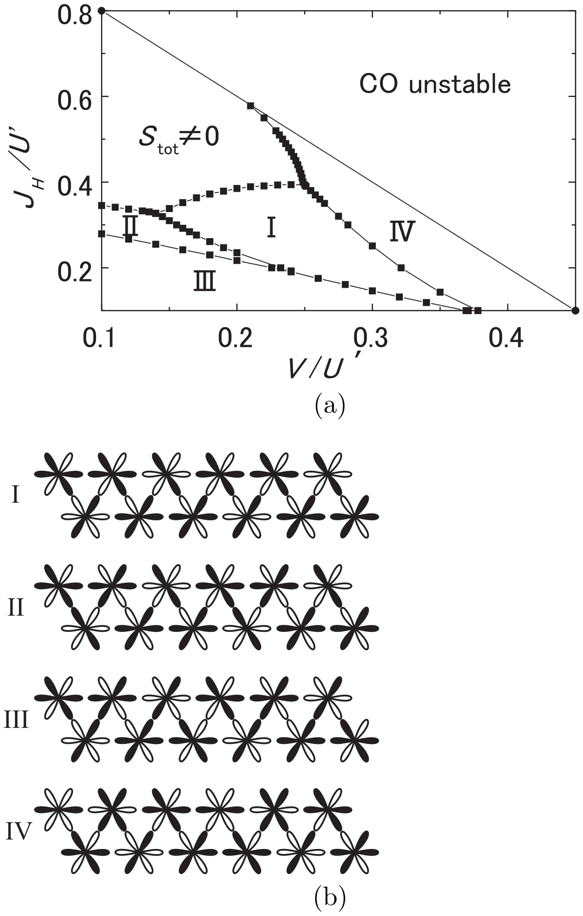

(a)

(b)

Fig. 5. (a) Calculated ground-state phase diagram of the effective spin-orbit Hamiltonian. The phases I–IV have the OO spatial patterns shown in (b). The region indicated as $S_{\mathrm{tot}} > 0$ has the OO pattern I but has higher total spins. The CO of V^{3+} and V^{4+} is unstable in the upper-right part of the phase diagram. (b) Calculated OO spatial patterns of the phases I–IV. Shaded lobes have the electrons.

§5. Phase diagram

Now, let us calculate the ground-state phase diagram of the effective Hamiltonian derived in the previous section. We use the 12-site (corresponding to 36-orbital) cluster with eight $S = 1$ spins and four $S = 1/2$ spins (corresponding to the filling of 20 electrons) coupled with the derived exchange interactions in the lattice of the CO pattern; we thereby calculated the ground state of each spin Hamiltonian. The periodic boundary condition is used. The calculated results for all possible OO patterns (where we assume the unit cell containing 6 sites) indicate that a variety of the OO patterns appear as the ground state, depending on the parameter values of J_H/U' and V/U' as shown in Fig. 5(a).

The OO spatial patterns of the phases I–IV are illustrated in Fig. 5(b). Careful inspection of the patterns indicate that the gain in kinetic energy by the process FM-3 is the most important to stabilize these phases. This is evident in Table I, where the numbers of types of bonds existing in the phases I–IV are listed; i.e., the OO patterns I–IV are stabilized by maximizing the number of the bond FM-3 where the constant c-value is predominantly lower than others as shown in Fig. 6(a).

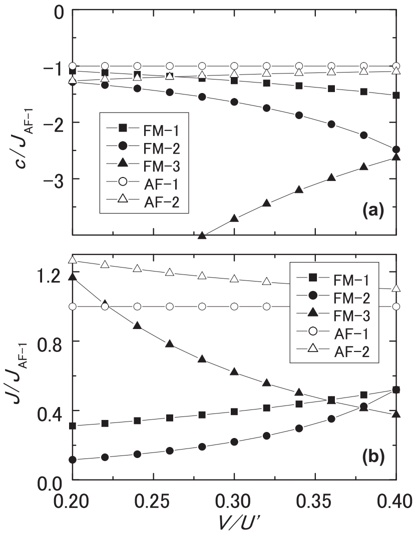

Fig.6 Y. Shibata and Y. Ohta

Fig. 6. Calculated values of (a) the exchange coupling constants J and (b) constant terms c in the effective spin Hamiltonians. The values normalized by the exchange coupling constant of the bond AF-1 are plotted.

We find in Fig. 6(b) that the exchange energies of the antiferromagnetic bonds are generally larger than the exchange energies of the ferromagnetic bonds; $J_{\mathrm{AF}} > J_{\mathrm{F}}$. This energy difference determines the detailed energy differences of the phases I–IV. For example, it may be that the strong AF-1 coupling promotes the singlet formation of the $S = 1$ spin pair by lowering its energy, to result in the appearance of the relatively stable phase I. Also, when the value of J_H is small, the strong antiferromagnetic couplings AF-1 and AF-2 stabilize the phase III as is noted in Table I. On the other hand, when J_H is large, the ferromagnetic couplings FM-1 and FM-2 stabilize the phase I as is also noted in Table I. When V/U' is small, the phase $S_{\mathrm{tot}} > 0$, which has the same OO pattern as the phase I, becomes the ground state. This may be due to the strong ferromagnetic coupling FM-3, which is rapidly enhanced when V/U' becomes small as we find in Fig. 6(b).

Because $J_H/U' \simeq 0.2$ in the real material but the value of V/U' is not well-known, we may expect that the phases I–IV should all be possible to be realized. However, the experimental data on the spin degrees of freedom may single out a possible phase as we will discuss in the next section.

§6. Discussion

Finally, let us discuss the spin degrees of freedom of the system. Speculated spin states of the phases I–IV are illustrated in Fig. 7, which is supported in part by our small-cluster calculations of the spin correlation functions for the spin Hamiltonians. We find that the variety of the OO patterns we have obtained result in a variety of the spin states as discussed below, although detailed numerical analyses of the Hamiltonians are needed for the definite descriptions of the states, which we leave for future study.

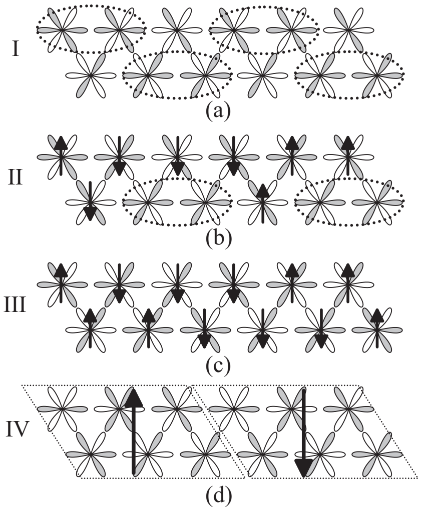

Fig. 7. Speculated spin states of the phases I–IV, where shaded lobes have the electrons, dotted circles represent the local spin-singlet state, and arrows indicate the spin direction. (a) Phase-I: Singlets of two $S = 1$ spins and nearly-free $S = 1/2$ spins coexist. (b) Phase-II: Intermediate state between phases I and III. (c) Phase-III: State without spin frustration and thus with strong AF spin correlation. (d) Phase-IV: AF state with local high-spin clusters.

For phase I, we find that the OO spatial pattern may be consistent with the spin state where the spin structure may be of the *partial* singlet formation; i.e., 2/3 of V-ions have $S = 1$ and form the spin singlet pairs, leaving $S = 1/2$ free spins on 1/3 of V-ions. For phase III, we find that the state has no spin frustration and thus we have the strong local antiferromagnetic spin correlations.

For phase II, we have the intermediate spin state between the phases I and III. For phase IV, we find that the state is formed by the local high-spin clusters of six V-ions, which are linked in the antiferromagnetic arrangement.

We may then suggest the following picture for the charge and orbital structure of the ground state of $\mathrm{Bi}_x\mathrm{V}_8\mathrm{O}_{16}$: (i) There occurs the CO where the V-ions order as $\cdots\mathrm{V}^{3+}\mathrm{V}^{3+}\mathrm{V}^{4+}\cdots$ in the chain direction. Thus, one should observe the crystal structure of three-fold periodicity. (ii) The possible spatial patterns of orbitals selected among the three t_{2g}-orbitals are determined as the phase I in Fig. 5(b). (iii) The spin degrees of freedom are then considered to be the partial singlet formation. This state may be consistent with the result of an NMR experiment recently made by Waki *et al.*,[7] where it has been suggested that most of the spins form the singlet state with leaving a small amount of active spins, which then undergo an additional phase transition into the magnetic long-range order at lower temperatures.

As for the MI phase transition of the real material, we suspect that the highly frustrated electronic state makes the system metallic at high temperatures, the CO occurs by lowering temperature to result in the MIT, and, triggered by this transition (but simultaneously), there occur the OO and spin-singlet formation. At lower temperatures, there appears the magnetic long-range order,[2] which may be due to the weak exchange coupling between the $S = 1/2$ spins in our OO system (though not considered in this paper).

The approximation used here neglects the orbital fluctuation completely. The effect may however be important if we want to consider, e.g., the state at finite temperatures. The use of the approximation may however be justified because we here want to answer the question "what is the ground-state OO pattern if we assume the presence of OO". Possible absence of OO as in LaTiO_3[8] may of course be an interesting issue in the present system as well. Jahn-Teller distortions as a mechanism of the phase transition might also be relevant. Further experimental (as well as theoretical) studies on the microscopic mechanism of this phase transition are therefore highly desirable.

§7. Summary

We have studied the electronic states of a vanadate material $\mathrm{Bi}_x\mathrm{V}_8\mathrm{O}_{16}$, a possibly new charge and orbital ordering system with the t_{2g}-orbitals on a 1D triangular lattice with the mixed valency of $3d^2 : 3d^1 = 2 : 1$. By assuming the charge ordering pattern, we have derived the effective spin-orbit Hamiltonian by the second-order perturbation theory. Within the approximation neglecting small off-diagonal hopping parameters, we have found that the Hamiltonian is block-diagonal with vanishing orbital-off-diagonal sectors. We then have used a numerical diagonalization technique on small clusters of this Hamiltonian and have found that a variety of the ground-state phases with different orbital ordering patterns appear in the parameter space. We have argued that the orbital ordering pattern possibly realized in experiment should be a state of the partial singlets where the nearest-neighbor spin $S = 1$ pairs form singlets with leaving the nearly free S=1/2 spins.

Although experimental data on this material are quite limited at present, we hope that the present theoretical study will encourage further experimental studies to clarify the nature of the charge, orbital, and spin degrees of freedom of this interesting material.

Acknowledgements

We would like to thank Prof. K. Yoshimura for enlightening discussion on the experimental aspects of $\mathrm{Bi}_x\mathrm{V}_8\mathrm{O}_{16}$. This work was supported in part by Grants-in-Aid for Scientific Research (Nos. 11640335 and 12046216) from the Ministry of Education, Science, Sports, and Culture of Japan. Computations were carried out at the computer centers of the Institute for Molecular Science, Okazaki, and the Institute for Solid State Physics, University of Tokyo.

---

1) See, e.g., Y. Tokura and N. Nagaosa: Science **288** (2000) 462.
2) H. Kato, T. Waki, M. Kato, K. Yoshimura and K. Kosuge: J. Phys. Soc. Jpn. **70** (2000) 325.
3) H. F. Pen, J. Brink, D. I. Khomskii and G. A. Sawatzky: Phys. Rev. Lett. **78** (1997) 1323.
4) H. F. Pen, L. H. Tjeng, E. Pellegrin, F. M. F. de Groot, G. A. Sawatzky, M. A. van Veenendaal and C. T. Chen: Phys. Rev. B **55** (1997) 15500.
5) K. I. Kugel and D. I. Khomskii: Sov. Phys.-JETP **37** (1973) 725; Sov. Phys. Usp. **25** (1982) 231, and references therein.
6) B. H. Brandow: Adv. Phys. **26** (1977) 651.
7) T. Waki, H. Kato, M. Kato and K. Yoshimura: Proceedings of ORBITAL-2001 and ISSP-Kashiwa 2001 (2001).
8) G. Khaliullin and S. Maekawa: Phys. Rev. Lett. **85** (2000) 3950.